

A Plasma α -Tocopherome Can Be Identified from Proteins Associated with Vitamin E Status in School-Aged Children of Nepal^{1–3}

Keith P West Jr.,^{4*} Robert N Cole,⁷ Sudeep Shrestha,⁴ Kerry J Schulze,⁴ Sun Eun Lee,⁴ Joshua Betz,⁵ Bareng AS Nonyane,⁴ Lee S-F Wu,⁴ James D Yager,⁶ John D Groopman,⁶ and Parul Christian⁴

Departments of ⁴International Health, ⁵Biostatistics, and ⁶Environmental Health Sciences, Center for Human Nutrition, Johns Hopkins University Bloomberg School of Public Health, Baltimore, MD; and ⁷Department of Biological Chemistry, Johns Hopkins School of Medicine Mass Spectrometry and Proteomics Facility, Baltimore, MD

Abstract

Background: The term vitamin E describes a family of 8 vitamers, 1 of which is α -tocopherol, that is essential for human health. Vitamin E status remains largely unknown in low-income countries because of the complexity and cost of measurement. Quantitative proteomics may offer an approach for identifying plasma proteins for assessing vitamin E status in these populations.

Objective: To improve options for vitamin E status assessment, we sought to detect and quantify a set of plasma proteins associated with α - and γ -tocopherol concentrations in a cohort of 500 rural Nepalese children aged 6–8 y and, based on nutrient-protein associations, to predict the prevalence of vitamin E deficiency (α -tocopherol <12 μ mol/L).

Methods: Study children were born to mothers enrolled in an earlier antenatal micronutrient trial in Sarlahi District, Nepal. Plasma α - and γ -tocopherol concentrations were measured by high-performance liquid chromatography. Plasma aliquots were depleted of 6 high-abundance proteins, digested with trypsin, labeled with isobaric mass tags, and assessed for relative protein abundance by tandem mass spectrometry. Linear mixed-effects models were used to evaluate the association between α -tocopherol status and relative protein abundance and to predict deficiency.

Results: We quantified 982 plasma proteins in >10% of all child samples, of which 119 correlated with α -tocopherol (false discovery rate, $q < 0.10$). Proteins were primarily involved in lipid transport, coagulation, repair, innate host defenses, neural function, and homeostasis. Six proteins [apolipoprotein (apo)C-III; apoB; pyruvate kinase, muscle; forkhead box O4; unc5 homolog C; and regulator of G-protein signaling 8] explained 71% of the variability in plasma α -tocopherol, predicting an in-sample population prevalence of vitamin E deficiency of 51.4% (95% CI: 46.4%, 56.3%) compared with a measured prevalence of 54.8%. Plasma γ -tocopherol was associated with 12 proteins ($q < 0.10$), 2 of which (apoC-III and Misato 1) explained 20% of its variability.

Conclusions: In this undernourished population of children in South Asia, quantitative proteomics identified a large plasma α -tocopherome from which 6 proteins predicted the prevalence of vitamin E deficiency. The findings illustrate that protein biomarkers, once absolutely quantified, can potentially predict micronutrient deficiencies in populations. The maternal micronutrient supplementation trial from which data were derived as a follow-up activity was registered with clinicaltrials.gov as NCT00115271. *J Nutr* 2015;145:2646–56.

Keywords: vitamin E, α -tocopherol, γ -tocopherol, tocopherome, plasma proteomics, bioinformatics, micronutrient assessment, Nepal

Introduction

Vitamin E is a collective term that refers to 2 groups of fat-soluble compounds that comprise 4 tocopherols (α , β , δ , γ) and 4 tocotrienols (α , β , δ , γ), of which 2 are of the greatest public

health importance: α -tocopherol, which is biologically most active in vivo and essential for human health, and γ -tocopherol, which is usually regarded to be most abundant in foods but less

¹ Supported by the plasma nutripoteomics study through the Assessment of Micronutrient Status by Nutripoteomics grant OPP 5241 from the Bill & Melinda Gates Foundation (Yiwu He, Senior Program Officer). The cohort study in Nepal from which plasma samples were obtained was supported by the Global Control of Micronutrient Deficiency grant GH 614 [also from the Bill & Melinda Gates Foundation (Ellen Piwoz, Senior Program Officer)]. The original field trial in Nepal from 1999 to 2001 in which mothers of studied children were enrolled was

supported by Micronutrients for Health Cooperative Agreement HRN-A-00-97-00015-00 between the Office of Health, Infectious Diseases and Nutrition, US Agency for International Development and the Center for Human Nutrition, Johns Hopkins Bloomberg School of Public Health. The Sight and Life Research Institute also provided additional technical assistance.

² Author disclosures: KP West Jr., RN Cole, S Shrestha, KJ Schulze, SE Lee, J Betz, BAS Nonyane, LS-F Wu, JD Yager, JD Groopman, and P Christian, no conflicts of interest.

well utilized in humans (1). In developing countries, where micronutrient deficiencies are endemic, vitamin E deficiency may be a public health problem, but it remains virtually unassessed. Although molecular mechanisms, functions, and clinical effects of varying vitamin E intakes through diet and supplementation represent active areas of research in high-income, often better-nourished societies, a review published in 2011 surprisingly found only 19 population-based assessments of vitamin E status published from low- to middle-income countries between 1992 and 2009 (11, 3, and 5 among children, the elderly, and groups of mixed ages, respectively). Based on a plasma α -tocopherol concentration cutoff that varied from 12 to 14 $\mu\text{mol/L}$, the prevalence of vitamin E deficiency ranged from 6% to 70%, 27% to 55%, and 4% to 70% in each of these population groups (2). Other recent population studies of women and school-aged children in Bangladesh and Nepal have revealed prevalences of $\sim 50\%$ and higher for α -tocopherol concentrations $<12 \mu\text{mol/L}$ (3, 4). A recent study in Bangladesh reported early-gestation vitamin E deficiency (plasma α -tocopherol $<12 \mu\text{mol/L}$) to be associated with a nearly 2-fold increased risk of miscarriage (5). This compilation of evidence suggests that vitamin E deficiency could be a major public health problem while revealing at the same time a gaping hole in knowledge about its extent, severity, and epidemiology for all ages in undernourished and nutrition-transitioning societies. Sparser yet are population data on γ -tocopherol status in low- to middle-income countries, for which health effects and an interpretation of circulating concentrations remain undefined.

A barrier to acquiring population data on vitamin E status relates to the difficulty and expense of measuring plasma or serum tocopherols by HPLC, which is the method of choice for assessing tocopherol concentrations but requires technical skills and resources often lacking in low-resource settings. As a result, biospecimens must be collected and typically transported in dry ice or liquid nitrogen to regional or global reference laboratories for vitamin E measurements, adding further costs and time for assessment (5). Suitable alternatives are needed for more rapid, less expensive, on-site assessments to accelerate the accrual of data for better assessing and understanding the extent to which vitamin E deficiency affects public health. A similar need exists for most other micronutrients (6). Identifying plasma proteins that are reliably associated with plasma concentrations of α -tocopherol and other micronutrients could pave the way for less expensive and more rapid field-based protein assays (e.g., with highly specific antibody panels that target sets of plasma proteins) to estimate multiple nutrient status distributions and to better target prevention efforts in the future.

We recently demonstrated that plasma proteomics offers a useful approach for identifying protein biomarkers for conventional micronutrient status indicators (7). The validity of plasma proteomics for assessing micronutrient status rests on 2 axioms: 1) that nutrients are absorbed, transported, metabolized, and interact—directly or through systemic metabolic circuits—through a vast set of proteins, and 2) that detectable plasma nutrient:protein associations reliably reflect systemic covariation under a wide range of health and disease states. Combining mass spectrometry, bioinformatics, and statistical modeling (8), we reported correlations between the plasma concentrations of 5 micronutrients (vitamins A, D, and E and copper and selenium) and relative abundance of 5 transport proteins for these nutrients

in Nepali children. In this proof-of-concept analysis, α -tocopherol was most strongly correlated with apoC-III ($r = 0.64$), a principal constituent of VLDLs (9) to which the vitamer is bound when secreted from the liver into circulation (10). This finding was consistent with a study of young Canadian adults, among whom apoC-III was 1 of 7 proteins most strongly associated with plasma α -tocopherol (11). We further derived a preliminary 2-protein model [apoC-III and regulator of G-protein signaling 8 (RGS8)⁸] that explained 65% of the variance in plasma α -tocopherol (7), suggesting that plasma proteins can potentially predict vitamin E status. This analysis extends preliminary findings to specify a large, chance-adjusted plasma α -tocopherome (proteins covarying with vitamin E status), offers a more complete model for predicting plasma α -tocopherol, and reports a smaller, less predictive plasma γ -tocopherome.

Methods

Field trial and cohort follow-up study. Subjects whose biospecimens were analyzed for this study were members of a cohort of 6- to 8-y-old children living in Sarlahi District, Nepal, whose mothers participated in a 5-arm antenatal micronutrient supplementation trial between 1999 and 2001 (12) and whose health and nutritional status were reexamined between 2006 and 2008. In that trial, women received 1 of 5 different supplements in recommended dietary allowance amounts (folic acid, iron-folic acid, iron-folic acid and zinc, a multiple micronutrient supplement, or placebo) from early pregnancy through 3 mo postpartum (12); in addition, a small proportion of the children ($\sim 8\%$) received either iron-folic acid or zinc supplements from 12 to 36 mo of age (4). During the follow-up, we assessed socioeconomic status, children's 7-d food frequencies and morbidity, and anthropometry by reported methods (13, 14). Venous blood was drawn, processed into plasma aliquots, shipped under vapor-phase liquid nitrogen, and stored at -80°C in the micronutrient analysis laboratory at Johns Hopkins University in Baltimore, Maryland (4). Informed consents were obtained during the original trial and follow-up study. All protocols were approved by institutional review boards in Kathmandu, Nepal, and at Johns Hopkins University. The original trial was registered with clinicaltrials.gov: NCT0011527. Reports on child health (13), growth (14), cognition (15), and micronutrient status (4) have appeared previously.

Micronutrient and proteomics study. In the original trial, 4998 mothers gave birth to 4130 infants, 3524 of whom were contacted at ages 6–8 y for follow-up. Venous blood was drawn from 3305 children; sufficient plasma existed for 2726. Complete trial-to-follow-up data and bioarchives were available for 2130 children, 200 of whom were randomly sampled from each original maternal supplement group to yield 1000 child plasma samples for micronutrient analyses, including α - and γ -tocopherol (4). From these 1000 samples, we randomly sampled 50% ($n = 100$ per original trial group) to obtain 500 specimens for protein analysis.

Plasma α - and γ -tocopherol analyses. Plasma α -tocopherol and γ -tocopherol were analyzed following the procedure of Yamini et al. (16) on a reverse-phase Waters Alliance 2795 HPLC system (Waters Corporation) with a quaternary gradient pump, autosampler, Waters 2996 photodiode array detector, and Empower 2 software (3, 4). Separation was achieved using a Supelcosil LC-18 column in combination with a LC-18 2-cm \times 4.0-mm guard column (Sigma-Aldrich). Tocopherols were assessed at 295 nm. The National Institute of Standards and Technology standard reference material SRM968d was used for calibration, with 3.7% and 8.6% coefficients of variation for α - and γ -tocopherol, respectively, across repeated runs of the reference

³ Supplemental Table 1 is available from the "Online Supporting Material" link in the online posting of the article and from the same link in the online table of contents at <http://jn.nutrition.org>.

*To whom correspondence should be sent. E-mail: kwest@jhsph.edu.

⁸ Abbreviations used: AIC, Akaike information criterion; LME, linear mixed effects; PKM, pyruvate kinase, muscle; RGS8, regulator of G-protein signaling 8; SERPING1, serine peptidase inhibitor, clade G, member 1.

TABLE 1 Plasma proteins positively associated with plasma α -tocopherol in children of rural Nepal aged 6–8 y (n = 500)¹

Protein name	HUGO gene symbol	n ²	r	R ²	P	q	b ₁ ³	Accession number ⁴
ApoC-III	<i>APOC3</i>	500	0.63	0.40	2.34×10^{-31}	3.19×10^{-28}	3.84	4557323
ApoB	<i>APOB</i>	500	0.60	0.37	3.28×10^{-24}	2.23×10^{-21}	5.67	105990532
ApoA-I	<i>APOA1</i>	500	0.57	0.32	4.91×10^{-17}	2.22×10^{-14}	5.34	4557321
ApoC-II	<i>APOC2</i>	500	0.56	0.32	4.03×10^{-16}	1.37×10^{-13}	2.70	32130518
ApoC-IV	<i>APOC4</i>	500	0.56	0.31	2.07×10^{-15}	5.61×10^{-13}	2.46	4502161
ApoM	<i>APOM</i>	500	0.56	0.31	3.94×10^{-15}	8.93×10^{-13}	4.88	22091452
Retinol-binding protein 4	<i>RBP4</i>	500	0.55	0.30	2.61×10^{-13}	5.06×10^{-11}	3.89	55743122
ApoA-II	<i>APOA2</i>	500	0.55	0.30	7.54×10^{-13}	1.28×10^{-10}	4.20	4502149
Proteoglycan 4 isoform D	<i>PRG4</i>	403	0.56	0.32	3.42×10^{-12}	5.16×10^{-10}	4.83	189181724
ApoC-I	<i>APOC1</i>	500	0.52	0.27	1.42×10^{-8}	1.92×10^{-6}	1.43	4502157
Interferon-related developmental regulator 2	<i>IFRD2</i>	486	0.53	0.28	1.55×10^{-8}	1.92×10^{-6}	2.64	197333755
ApoE	<i>APOE</i>	500	0.52	0.27	8.40×10^{-8}	8.79×10^{-6}	3.02	4557325
Kinesin-like protein KIF20B	<i>KIF20B</i>	326	0.54	0.29	1.56×10^{-7}	1.51×10^{-5}	2.80	46049114
Transthyretin	<i>TTR</i>	500	0.52	0.27	1.93×10^{-7}	1.75×10^{-5}	3.95	4507725
ApoD	<i>APOD</i>	500	0.51	0.26	9.98×10^{-7}	7.18×10^{-5}	2.61	4502163
Paraoxonase 1	<i>PON1</i>	500	0.51	0.26	3.03×10^{-6}	1.86×10^{-4}	2.14	19923106
Cathelicidin antimicrobial peptide	<i>CAMP</i>	417	0.52	0.27	3.43×10^{-6}	1.86×10^{-4}	1.75	39753970
Unc5 homolog C	<i>UNC5C</i>	139	0.59	0.35	5.63×10^{-6}	2.83×10^{-4}	3.13	16933525
Kruppel-like factor 17	<i>KLF17</i>	284	0.53	0.28	6.24×10^{-6}	3.03×10^{-4}	1.99	104294874
Protein C	<i>PROC</i>	500	0.51	0.26	7.71×10^{-6}	3.49×10^{-4}	3.12	4506115
Chromosome 4 open reading frame 22	<i>C4orf22</i>	138	0.62	0.38	1.05×10^{-5}	4.59×10^{-4}	2.94	22749509
Insulin-like growth factor-binding protein 3 isoform b	<i>IGFBP3</i>	500	0.51	0.26	1.44×10^{-5}	6.13×10^{-4}	1.98	62243068
Misato homolog 1	<i>MSTO1</i>	110	0.59	0.35	2.33×10^{-5}	9.32×10^{-4}	3.92	39780571
Insulin-like growth factor-binding protein, acid-labile subunit isoform 2	<i>IGFALS</i>	500	0.50	0.25	3.43×10^{-5}	1.29×10^{-3}	2.03	4826772
Carnosine dipeptidase	<i>CNDP1</i>	500	0.50	0.25	1.41×10^{-4}	4.40×10^{-3}	1.10	21071039
Forkhead box protein O4	<i>FOXO4</i>	70	0.58	0.33	1.42×10^{-4}	4.40×10^{-3}	3.20	103472003
Aldehyde dehydrogenase 9A1	<i>ALDH9A1</i>	90	0.58	0.33	2.62×10^{-4}	7.76×10^{-3}	1.79	115387104
TATA element modulatory factor	<i>TMF1</i>	243	0.53	0.28	3.43×10^{-4}	9.52×10^{-3}	1.92	110347443
Afamin	<i>AFM</i>	500	0.50	0.25	3.87×10^{-4}	1.01×10^{-2}	2.16	4501987
Kallikrein B, plasma 1	<i>KLKB1</i>	500	0.50	0.25	4.26×10^{-4}	1.07×10^{-2}	3.00	78191798
Golgin B1	<i>GOLGB1</i>	348	0.50	0.25	6.24×10^{-4}	1.47×10^{-2}	1.87	148596984
ApoL1 isoform c	<i>APOL1</i>	500	0.50	0.25	1.19×10^{-3}	2.44×10^{-2}	1.68	211938442
Coagulation factor XI	<i>F11</i>	500	0.50	0.25	1.22×10^{-3}	2.44×10^{-2}	2.32	4503627
Keratin 74	<i>KRT74</i>	140	0.52	0.27	1.52×10^{-3}	2.75×10^{-2}	2.21	148612803
Eukaryotic translation initiation factor 2D	<i>EIF2D</i>	256	0.51	0.26	1.56×10^{-3}	2.80×10^{-2}	1.92	56699485
Cystic fibrosis transmembrane conductance regulator	<i>CFTR</i>	70	0.51	0.26	1.63×10^{-3}	2.84×10^{-2}	5.04	90421313
Hornerin	<i>HRNR</i>	291	0.47	0.22	1.70×10^{-3}	2.93×10^{-2}	0.93	57864582
Coagulation factor XIII, A1 polypeptide	<i>F13A1</i>	500	0.50	0.25	1.88×10^{-3}	3.19×10^{-2}	2.38	119395709
Secretoglobin family 3A, member 1	<i>SCGB3A1</i>	298	0.49	0.24	2.16×10^{-3}	3.59×10^{-2}	1.06	50363226
Clathrin, heavy chain	<i>CLTC</i>	181	0.54	0.29	2.28×10^{-3}	3.73×10^{-2}	1.47	4758012
Heat shock 90-kDa protein α (cytosolic), class B member 1	<i>HSP90AB1</i>	193	0.53	0.28	2.60×10^{-3}	4.20×10^{-2}	1.62	20149594
Paraoxonase 3	<i>PON3</i>	493	0.49	0.24	2.96×10^{-3}	4.74×10^{-2}	1.65	29788996
Albumin	<i>ALB</i>	500	0.50	0.25	3.71×10^{-3}	5.55×10^{-2}	0.36	4502027
Selenoprotein P, plasma 1	<i>SEPP1</i>	500	0.50	0.25	3.90×10^{-3}	5.76×10^{-2}	1.69	62530391
Keratin 9	<i>KRT9</i>	500	0.50	0.25	4.47×10^{-3}	6.30×10^{-2}	0.68	55956899
Poly(ADP-ribose) glycohydrolase	<i>PARG</i>	139	0.50	0.25	4.54×10^{-3}	6.30×10^{-2}	1.87	70610136
Cyclin B3	<i>CCNB3</i>	125	0.49	0.24	4.90×10^{-3}	6.56×10^{-2}	1.88	90669307
Galactosidase, β 1-like	<i>GLB1L</i>	104	0.56	0.31	4.93×10^{-3}	6.56×10^{-2}	3.02	40255043
Keratin 1	<i>KRT1</i>	500	0.50	0.25	5.45×10^{-3}	6.98×10^{-2}	0.67	119395750
Coagulation factor II (thrombin)	<i>F2</i>	500	0.50	0.25	6.31×10^{-3}	7.51×10^{-2}	2.93	4503635
Rap guanine nucleotide exchange factor 5	<i>RAPGEF5</i>	132	0.45	0.20	7.44×10^{-3}	8.57×10^{-2}	0.75	119392077
FK506-binding protein 1A, 12 kDa	<i>FKBP1A</i>	105	0.49	0.24	7.53×10^{-3}	8.60×10^{-2}	1.40	17149836
Integrin, α 5	<i>ITGA5</i>	63	0.64	0.40	7.64×10^{-3}	8.65×10^{-2}	4.44	56237029
Zinc finger and BTB domain containing 1	<i>ZBTB1</i>	119	0.43	0.19	7.77×10^{-3}	8.70×10^{-2}	2.43	182509178
ApoA-IV	<i>APOA4</i>	500	0.50	0.25	8.60×10^{-3}	9.28×10^{-2}	1.23	71773110
Glycosylphosphatidylinositol-specific phospholipase D1	<i>GPLD1</i>	500	0.50	0.25	8.85×10^{-3}	9.41×10^{-2}	1.73	29171717
Protein Z, vitamin K-dependent plasma glycoprotein	<i>PROZ</i>	500	0.50	0.25	9.27×10^{-3}	9.55×10^{-2}	0.97	4506121
Coagulation factor XIII, B polypeptide	<i>F13B</i>	500	0.50	0.25	9.47×10^{-3}	9.61×10^{-2}	2.26	110611237

(Continued)

TABLE 1 Continued

Protein name	HUGO gene symbol	n^2	r	R^2	P	q	b_1^3	Accession number ⁴
Bardet-Biedl syndrome 7	<i>BBS7</i>	153	0.38	0.14	9.90×10^{-3}	9.83×10^{-2}	2.03	29029555
Melanoma antigen family B3 pseudogene	<i>LOC392435</i>	312	0.50	0.25	9.98×10^{-3}	9.83×10^{-2}	2.20	169216998
Coagulation factor VII	<i>F7</i>	472	0.49	0.24	1.02×10^{-2}	9.85×10^{-2}	1.77	10518503

¹ Sixty-two proteins quantified by mass spectrometry and estimated by LME modeling in >10% of the samples that were positively correlated with plasma α -tocopherol ($P < 0.01$, $q < 0.10$), listed in increasing order of q , defined as positively associated protein biomarkers of a plasma α -tocopherome. HUGO, Human Genome Organization; LME, linear mixed effects.

² Number (n) of child plasma samples in which a protein was detected and quantified by iTRAQ tandem mass spectrometry (excludes subsequent imputations required for multivariable LME models).

³ Univariate LME-modeled positive slope indicating change in plasma α -tocopherol concentration (in $\mu\text{mol/L}$) per 100% increase in relative abundance of each listed plasma protein.

⁴ GenInfo sequence number as assigned to all nucleotide and protein sequences by the National Center for Biotechnology Information at the National Library of Medicine, NIH (18).

material. Total cholesterol and TGs had previously been measured (Cholestech) (13).

Plasma proteomics analysis. Procedures developed for this study have been described (6). Briefly, 500 plasma samples were 85–90% immune-depleted of 6 high-abundance proteins (albumin, immunoglobulins G and A, transferrin, haptoglobin, and antitrypsin) using the Multiple Affinity Removal LC Column Human 6 system (Agilent Technologies). Protein extracts (100 μg each) were precipitated with tricarboxylic acid/acetone, digested with trypsin, labeled with an iTRAQ reagent (Sigma-Aldrich), fractionated by strong cation exchange chromatography, and analyzed on an LTQ Orbitrap Velos mass spectrometer (Thermo Fisher Scientific) in experiments that consisted of 7 samples plus 1 pooled sample for quality control and the random assignment of a unique iTRAQ reagent to each sample. The pooled sample was later found to be unnecessary for quantifying or normalizing data from multiple iTRAQ experiments (8). Tandem mass spectra were extracted and searched against the RefSeq 40 database using Mascot (Matrix Science) through Proteome Discoverer software version 1.3 (Thermo Fisher Scientific) to quantify proteins with respect to the within-iTRAQ medians of \log_2 -transformed and normalized reporter ion intensities derived from Proteome Discoverer (7, 8). Data were obtained from 72 iTRAQ experiments with an average of 589 proteins ($\text{SD} = 65$) quantified per experiment. In all, 4705 proteins were detected, with 982 quantified in >10% ($n > 50$) of all samples (7) and 146 proteins measured in all samples, representing the analyzed plasma proteome for this study.

Statistical analysis. General characteristics of study children were expressed as mean \pm SD or median (IQR) for continuous variables and percentage per category for discrete variables. Plasma α - and γ -tocopherol distributions that were skewed to the right were corrected with natural \log_2 transformations. For α -tocopherol, the \log_2 -transformed (7) and untransformed distributions revealed virtually the same results; thus, for simplicity, only untransformed α -tocopherol analyses are presented. Because the skew was more pronounced for plasma γ -tocopherol, results from the \log_2 -transformed γ -tocopherol analysis are presented.

Linear mixed-effects (LME) models were fitted via restricted maximum likelihood estimation procedures that combined complete proteomics data across all 72 iTRAQ experiments as previously described (7, 8). This model produced the following expected values of α - and \log_2 γ -tocopherol concentrations for each individual protein:

$$E\{N_{rk}\} = b_0 + B_r + b_1 P_{rk} \quad (1)$$

where N_{rk} denotes the observed (for α -tocopherol) or \log_2 -transformed (for γ -tocopherol) plasma nutrient concentration, k is the index for each sample in each r iTRAQ experiment, and P_{rk} is the relative abundance for each protein for each vitamer analysis. The parameter estimate b_0 is the intercept that is the overall mean concentration of each tocopherol; B_r denotes the random deviation from this mean in experiment r ; and b_1 estimates the slope of the nutrient:protein association, denoting absolute (in $\mu\text{mol/L}$) and relative (%) changes in

α - and γ -tocopherol, respectively, per 100% increase in relative abundance of each protein. Statistical significance of a protein-nutrient association was assessed via a 2-sided hypothesis test for $b_1 = 0$.

To account for multiple comparisons, a q value, which is a chance-adjusted P value that represents a false discovery rate (17), is reported for each single protein-nutrient association. All proteins classified into a plasma α - or γ -tocopherol proteome ($n = 119$ and 12, respectively) were required to meet a false discovery rate threshold of $q < 0.10$. Summary tables were generated separately for positively and negatively associated proteins for α -tocopherol and combined for γ -tocopherol, providing for each protein its respective Human Genome Organization gene symbol (18), number of measured protein values, protein:nutrient correlation (r), variance in nutrient concentration explained by the protein (R^2), q , the slope (b_1) with an associated P value for the test of $b_1 = 0$, and GenInfo identifier accession number (19).

Before fitting a multiple protein regression model for predicting vitamin E status, missing protein values in the database were imputed (20) employing a regression-based approach that assumed that the nutrient-protein relation observed in the complete data set could be used to infer missing protein values. Thus, for each vitamer and protein in their proteome (i.e., $n = 119$ and 12 for α - and γ -tocopherol, respectively), protein relative abundance values were regressed on nutrient concentration and predicted values from this regression were used to impute missing values. This imputation was conducted 10 times for each nutrient based on the assumption that this number of imputations would suffice to account for the variability among imputed values (differences in individual estimates derived from the analysis of each imputed dataset). The LME model was fitted to each of the imputed data sets, and the averages of the 10 model estimates, adjusted for between- and within-imputation variance, were adopted as the final model estimates.

The ability of plasma proteins to predict vitamin E status was explored using the combined dataset of measured and imputed protein values. This involved fitting a single multiple-protein model, built for each of the 2 vitamers E, by a forward stepwise inclusion procedure based on the variable inclusion P value criterion that started with the protein exhibiting the lowest q value in the single-protein LME models and allowing the model to select additional covariates from a set of proteins singly associated with each vitamer with a $q < 0.10$ and $P < 0.0001$. The Akaike information criterion (AIC), which is a function of the model likelihood, the number of parameters in the model (21, 22), and the likelihood test P value for $b_1 = 0$, were used to assess model fit and complexity. Lower values of the AIC indicate a relative improvement in model fit and better external validity (21). Stepwise inclusion of the protein with the smallest P value continued until no protein from each vitamer-specific set could reduce the AIC by ≥ 30 . In an effort to discover additional potential predictors, a second tier of protein candidates was identified for future consideration and population testing by repeating a series of forward stepwise procedures for proteins meeting either $q < 0.1$ or $q < 0.01$ criteria that excluded protein covariates fitted to each preceding model until no additional proteins met the above AIC criterion. Data analyses were carried out using in-house-developed open-source software implemented in the statistical environment R (23).

TABLE 2 Plasma proteins negatively associated with plasma α -tocopherol in children of rural Nepal aged 6–8 y ($n = 500$)¹

Protein name	HUGO gene symbol	n^2	r	R^2	P	q	b_1^3	Accession number ⁴
Cadherin 1, type 1	<i>CDH</i>	374	−0.53	0.28	6.87×10^{-8}	7.78×10^{-6}	−2.71	4757960
CD44 antigen isoform 4	<i>CD44</i>	486	−0.51	0.26	3.86×10^{-7}	3.28×10^{-5}	−3.11	48255941
Leucine-rich α -2-glycoprotein 1	<i>LRG1</i>	500	−0.51	0.26	4.79×10^{-7}	3.83×10^{-5}	−2.27	16418467
Ecotropic viral integration site 5	<i>EVI5</i>	271	−0.60	0.36	1.00×10^{-6}	7.18×10^{-5}	−2.21	68299759
NOP2/Sun domain family, member 6	<i>NSUN6</i>	249	−0.52	0.27	3.24×10^{-6}	1.86×10^{-4}	−2.44	32698918
Orosomucoid 1	<i>ORM1</i>	500	−0.51	0.26	3.55×10^{-6}	1.86×10^{-4}	−1.86	167857790
TNFAIP3-interacting protein 1	<i>TNIP1</i>	388	−0.50	0.25	6.96×10^{-6}	3.26×10^{-4}	−2.13	116256481
Serpin peptidase inhibitor, clade A, member 7	<i>SERPINA7</i>	500	−0.51	0.26	1.52×10^{-5}	6.25×10^{-4}	−3.17	205277441
Proteoglycan 2	<i>PRG2</i>	382	−0.48	0.23	3.37×10^{-5}	1.29×10^{-3}	−1.27	46276889
Quiescin Q6 sulfhydryl oxidase 1	<i>QSOX1</i>	500	−0.51	0.26	4.53×10^{-5}	1.66×10^{-3}	−4.83	13325075
γ -Glutamyl hydrolase	<i>GGH</i>	458	−0.49	0.24	7.54×10^{-5}	2.63×10^{-3}	−2.21	4503987
Intercellular adhesion molecule 2	<i>ICAM2</i>	451	−0.50	0.25	8.24×10^{-5}	2.80×10^{-3}	−2.85	153082722
Complement component 9	<i>C9</i>	500	−0.50	0.25	1.10×10^{-4}	3.66×10^{-3}	−2.20	4502511
β -2-Microglobulin	<i>B2M</i>	493	−0.50	0.25	1.32×10^{-4}	4.26×10^{-3}	−1.68	4757826
Pyruvate kinase, muscle	<i>PKM</i>	55	−0.63	0.40	2.11×10^{-4}	6.38×10^{-3}	−5.67	33286422
Leucine-rich repeat containing 47	<i>LRRC47</i>	70	−0.61	0.38	3.32×10^{-4}	9.40×10^{-3}	−5.94	24308207
Serpin peptidase inhibitor, clade A, member 3	<i>SERPINA3</i>	500	−0.50	0.25	3.83×10^{-4}	1.01×10^{-2}	−2.48	50659080
ARP actin-related protein 5 homolog	<i>ACTR5</i>	255	−0.54	0.29	5.19×10^{-4}	1.26×10^{-2}	−1.52	151301041
Orosomucoid 2	<i>ORM2</i>	500	−0.50	0.25	6.29×10^{-4}	1.47×10^{-2}	−1.92	4505529
Lymphocyte cytosolic protein 1 (L-plastin)	<i>LCP1</i>	500	−0.50	0.25	6.88×10^{-4}	1.53×10^{-2}	−2.84	167614506
Component of oligomeric golgi complex 3	<i>COG3</i>	215	−0.46	0.21	7.89×10^{-4}	1.70×10^{-2}	−1.68	13899251
Fc fragment of IgG, low-affinity IIIa, receptor (CD16a)	<i>FCGR3A</i>	202	−0.53	0.28	8.76×10^{-4}	1.86×10^{-2}	−1.27	189083842
Nucleolar protein with MIF4G domain 1	<i>NOM1</i>	119	−0.57	0.33	1.24×10^{-3}	2.44×10^{-2}	−1.88	61097912
Complement factor I	<i>CFI</i>	500	−0.50	0.25	1.30×10^{-3}	2.52×10^{-2}	−2.73	119392081
Timeless circadian clock	<i>TIMELESS</i>	133	−0.54	0.30	1.35×10^{-3}	2.59×10^{-2}	−4.24	222136585
Transforming growth factor, β -induced, 68 kDa	<i>TGFB1</i>	493	−0.50	0.25	1.42×10^{-3}	2.68×10^{-2}	−2.75	4507467
von Willebrand factor	<i>VWF</i>	500	−0.50	0.25	1.51×10^{-3}	2.75×10^{-2}	−1.73	89191868
Regulator of G-protein signaling 8	<i>RGS8</i>	56	−0.65	0.42	1.62×10^{-3}	2.84×10^{-2}	−1.15	156416024
Filamin C, γ	<i>FLNC</i>	175	−0.57	0.33	1.90×10^{-3}	3.19×10^{-2}	−0.59	188595687
Inter- α -tocopherol- γ -hydroxylase heavy chain family, member 4	<i>ITI4</i>	500	−0.50	0.25	3.13×10^{-3}	4.81×10^{-2}	−3.11	31542984
Inter- α -tocopherol- γ -hydroxylase heavy chain 3	<i>ITI3</i>	500	−0.50	0.25	4.12×10^{-3}	6.03×10^{-2}	−1.60	133925809
Insulin-like growth factor-binding protein 2, 36 kDa	<i>IGFBP2</i>	500	−0.50	0.25	4.18×10^{-3}	6.05×10^{-2}	−1.38	55925576
Heat shock 70-kDa protein 1-like	<i>HSPA1L</i>	278	−0.47	0.23	4.44×10^{-3}	6.30×10^{-2}	−1.74	124256496
Complement factor B	<i>CFB</i>	500	−0.50	0.25	4.53×10^{-3}	6.30×10^{-2}	−1.93	67782358
Fetuin B	<i>FETUB</i>	500	−0.50	0.25	4.63×10^{-3}	6.35×10^{-2}	−2.20	58331240
Dynein, axonemal, assembly factor 1	<i>DNAAF1</i>	207	−0.55	0.30	4.73×10^{-3}	6.42×10^{-2}	−1.54	157674358
Complement component 2	<i>C2</i>	423	−0.49	0.24	5.05×10^{-3}	6.67×10^{-2}	−3.22	14550407
Carboxypeptidase Q	<i>CPQ</i>	271	−0.50	0.25	5.22×10^{-3}	6.77×10^{-2}	−2.18	7706387
α -1-B glycoprotein	<i>A1BG</i>	500	−0.50	0.25	5.23×10^{-3}	6.77×10^{-2}	−2.85	21071030
Zinc finger, ZZ-type with EF-hand domain 1	<i>ZZEF1</i>	444	−0.51	0.26	5.54×10^{-3}	7.04×10^{-2}	−0.72	73747881
Sex hormone-binding globulin	<i>SHBG</i>	486	−0.50	0.25	5.61×10^{-3}	7.06×10^{-2}	−1.16	7382460
Lipocalin 2	<i>LCN2</i>	270	−0.52	0.27	5.67×10^{-3}	7.07×10^{-2}	−1.26	38455402
Vascular cell adhesion molecule 1	<i>VCAM1</i>	341	−0.50	0.25	5.81×10^{-3}	7.13×10^{-2}	−2.62	4507875
Serpin peptidase inhibitor, clade G, member 1	<i>SERPING1</i>	500	−0.50	0.25	6.20×10^{-3}	7.51×10^{-2}	−2.47	73858570
Chromogranin A	<i>CHGA</i>	340	−0.49	0.24	6.35×10^{-3}	7.51×10^{-2}	−1.30	4502805
Peroxisomal protein 2	<i>PRDX2</i>	486	−0.50	0.25	7.26×10^{-3}	8.50×10^{-2}	−0.58	32189392
Kininogen 1	<i>KNG1</i>	500	−0.50	0.25	7.31×10^{-3}	8.50×10^{-2}	−1.46	4504893
Haptoglobin	<i>HP</i>	354	−0.54	0.29	7.99×10^{-3}	8.78×10^{-2}	−0.37	4826762
Charcot–Leyden crystal protein	<i>CLC</i>	409	−0.50	0.25	8.01×10^{-3}	8.78×10^{-2}	−0.51	20357559
Ceruloplasmin (ferroxidase)	<i>CP</i>	500	−0.50	0.25	8.86×10^{-3}	9.41×10^{-2}	−2.29	4557485
Group-specific component (vitamin D-binding protein)	<i>GC</i>	500	−0.50	0.25	8.95×10^{-3}	9.43×10^{-2}	−3.01	32483410
Angiogenin, ribonuclease, RNase A family, 5	<i>ANG</i>	151	−0.43	0.18	9.19×10^{-3}	9.55×10^{-2}	−1.88	148277046
CD14 molecule	<i>CD14</i>	500	−0.50	0.25	9.22×10^{-3}	9.55×10^{-2}	−2.30	4557417
Desmoglein 2	<i>DSG2</i>	354	−0.49	0.24	9.43×10^{-3}	9.61×10^{-2}	−1.49	116534898
Prostaglandin D2 synthase 21 kDa (brain)	<i>PTGDS</i>	424	−0.49	0.24	9.77×10^{-3}	9.83×10^{-2}	−1.62	32171249

(Continued)

TABLE 2 *Continued*

Protein name	HUGO gene symbol	n^2	r	R^2	P	q	b_1^3	Accession number ⁴
Hemoglobin, $\alpha 1$	<i>HBA1</i>	486	-0.50	0.25	9.85×10^{-3}	9.83×10^{-2}	-0.36	4504347
Thioredoxin	<i>TXN</i>	311	-0.48	0.23	1.02×10^{-2}	9.85×10^{-2}	-1.22	50592994
Tubulin tyrosine ligase-like family, member 8	<i>TTL8</i>	293	-0.53	0.28	1.02×10^{-2}	9.85×10^{-2}	-1.49	122937293

¹ Fifty-nine proteins quantified by mass spectrometry and estimated by LME modeling in >10% of the samples that were negatively correlated with plasma α -tocopherol ($P < 0.01$, $q < 0.10$), listed in increasing order of q , defined as negatively associated protein biomarkers of a plasma α -tocopherome. HUGO, Human Genome Organization; IgG, immunoglobulin G; LME, linear mixed effects; MIF4G, middle domain of eukaryotic initiation factor 4G.

² Number (n) of child plasma samples in which a protein was detected and quantified by iTRAQ mass spectrometry (excludes subsequent imputations required for multivariable LME models).

³ Univariate LME-modeled negative slope indicating change in plasma α -tocopherol concentration (in $\mu\text{mol/L}$) per 100% increase in relative abundance of each listed plasma protein.

⁴ GenInfo sequence number as assigned to all nucleotide and protein sequences by the National Center for Biotechnology Information at the National Library of Medicine, NIH (18).

Results

Study children were moderately underweight, stunted, and thin, with 48%, 39%, and 16% below -2 z scores of the WHO international anthropometric weight-for-age, height-for-age, and body mass index-for-age references, respectively (24). Children in this sample were comparable in nutritional status to the larger sample of children who underwent micronutrient analysis (4) (Supplemental Table 1). Except for dairy (i.e., local yogurt), few children regularly consumed (≥ 3 times in past week) foods of animal origin, reflecting the usual diet in this region (25). Few children (3–8%) reported symptoms of illness in the previous 7 d. Plasma α -tocopherol concentrations (mean \pm SD) were 12.1 ± 3.2 $\mu\text{mol/L}$, with 54.8% (95% CI: 50.4, 59.2) of children being deficient (<12 $\mu\text{mol/L}$) (1, 26) and 17.6% (95% CI: 14.2, 21.0) having values <9.3 $\mu\text{mol/L}$, a suggested cutoff for moderate or worse vitamin E deficiency (3, 4). Plasma γ -tocopherol concentrations were lower (1.50 ± 0.68 $\mu\text{mol/L}$). Total cholesterol and TG concentrations were also low, with median (IQR) values of 2.87 mmol/L (2.59–3.28) and 1.00 mmol/L (0.75–1.33), respectively, justifying reporting vitamin E status without adjusting for plasma lipids (1).

Based on single-protein LME models, 119 proteins were associated with plasma α -tocopherol (all $q < 0.10$). Sixty-one proteins were positively correlated with α -tocopherol (Table 1), most notably aposA–C, E, and L. Positive correlates also included multifunctional proteins involved in vascular lipid, vitamin, mineral, and hormonal transport [retinol-binding protein 4, APOsD and M (27), transthyretin (28), insulin-like growth factor-binding protein 3, insulin-like growth factor acid-labile subunit, and selenoprotein P isoform 1 (29)].

Others included proteins that are active in innate immunity [cathelicidin antimicrobial peptide (30)], coagulation [factors XI, XIII (A1 and B polypeptides), II (thrombin), and VII and proteins C (31) and Z (32)], neuronal signaling [kinesin-like protein KIF20B (33), the netrin receptor unc5 homolog C (34), and transthyretin (35)], and redox homeostasis [paraoxonase 1 and 3 (36)]. The strongest positive associations with plasma α -tocopherol occurred with aposB, A-1, and M, with slopes (b_1) of 4.88–5.66 $\mu\text{mol/L}$ per 100% increase in relative protein abundance (Table 1).

Fifty-eight plasma proteins were negatively correlated with α -tocopherol (Table 2) including nutrient transporters [ceruloplasmin (37) and vitamin D-binding protein (38)] and proteins involved in cross-talking systems of hemostasis [von Willebrand factor (39)], innate immunity [complements 2 and 9, complement factors B and 1 (40), α_1 -acid glycoprotein isoforms of orosomucoid 1 and 2 (41), soluble CD14 coreceptor of toll-like

receptor 4 (42), and transforming growth factor 1 (43)], and cell and extracellular matrix adhesion [cadherin (44), CD44 antigen (45), intercellular and vascular cell adhesion molecules 2 and 1, respectively (46), and desmoglein (47)]. The α -tocopherol level was also negatively correlated with proteins involved in anticoagulative control [serine peptidase inhibitor, clade G, member 1 (SERPING1), also known as C1-inh (48)], neuronal [serpin peptidase inhibitor, clade A, member 3, known as α_1 -antichymotrypsin (49)] and red blood cell [haptoglobin and hemoglobin subunit $\alpha 1$ (50)] responses to inflammation, and redox homeostasis [ceruloplasmin (37), quiescin Q6 sulfhydryl oxidase 1 (51), periredoxin-2 (52), and thioredoxin (53)]. The strongest negative relations with plasma α -tocopherol were observed with leucine-rich repeat 47; pyruvate kinase, muscle (PKM); and quiescin Q6 sulfhydryl oxidase 1, with slopes (b_1) ranging from -5.97 to -4.83 $\mu\text{mol/L}$ per 100% change in protein relative abundance.

A correlation (r) matrix of 44 proteins in the plasma α -tocopherome, restricted to $q < 0.01$ and where r is re-expressed as $r \times 10^2$ to enable visualization (Figure 1) revealed highly variable protein-protein correlations with estimates ranging from 0.16 to 0.93 and -0.13 to -0.85 , reflecting a diverse proteome that can potentially predict vitamin E status.

Using the forward stepwise approach of building a multivariable LME model starting with the most predictive protein, we built a model with the following 6 proteins, each of which met the criteria of having the smallest P value, a q value <0.1 , and through its inclusion reducing the model AIC by at least 30 units: aposC-II and B, PKM, forkhead box 04, unc5 homolog C, and RGS8, accounting for 71% of variability in plasma α -tocopherol (Table 3).

Within this population sample, the 6-protein model predicted prevalences of vitamin E deficiency (α -tocopherol <12 $\mu\text{mol/L}$) (1, 26) and moderate or worse deficiency (<9.3 $\mu\text{mol/L}$) (3, 4) of 51.4% (95% CI: 46.4, 56.3) and 12.7% (CI: 8.9, 16.4) compared with measured prevalences of 54.8% and 17.6%, respectively. Additional analyses identified a second tier of 9 proteins that, although not in the model because of collinearity with the first 6, explained additional variability in α -tocopherol (see Table 3 footnote).

Twelve plasma proteins were associated with the log₂-transformed γ -tocopherol distribution ($q < 0.10$) (Table 4). Modeling these proteins after imputation identified 2 covariates (apoC-III and Misato homolog 1), explaining only 20% of the variability in γ -tocopherol and thus insufficient for prediction.

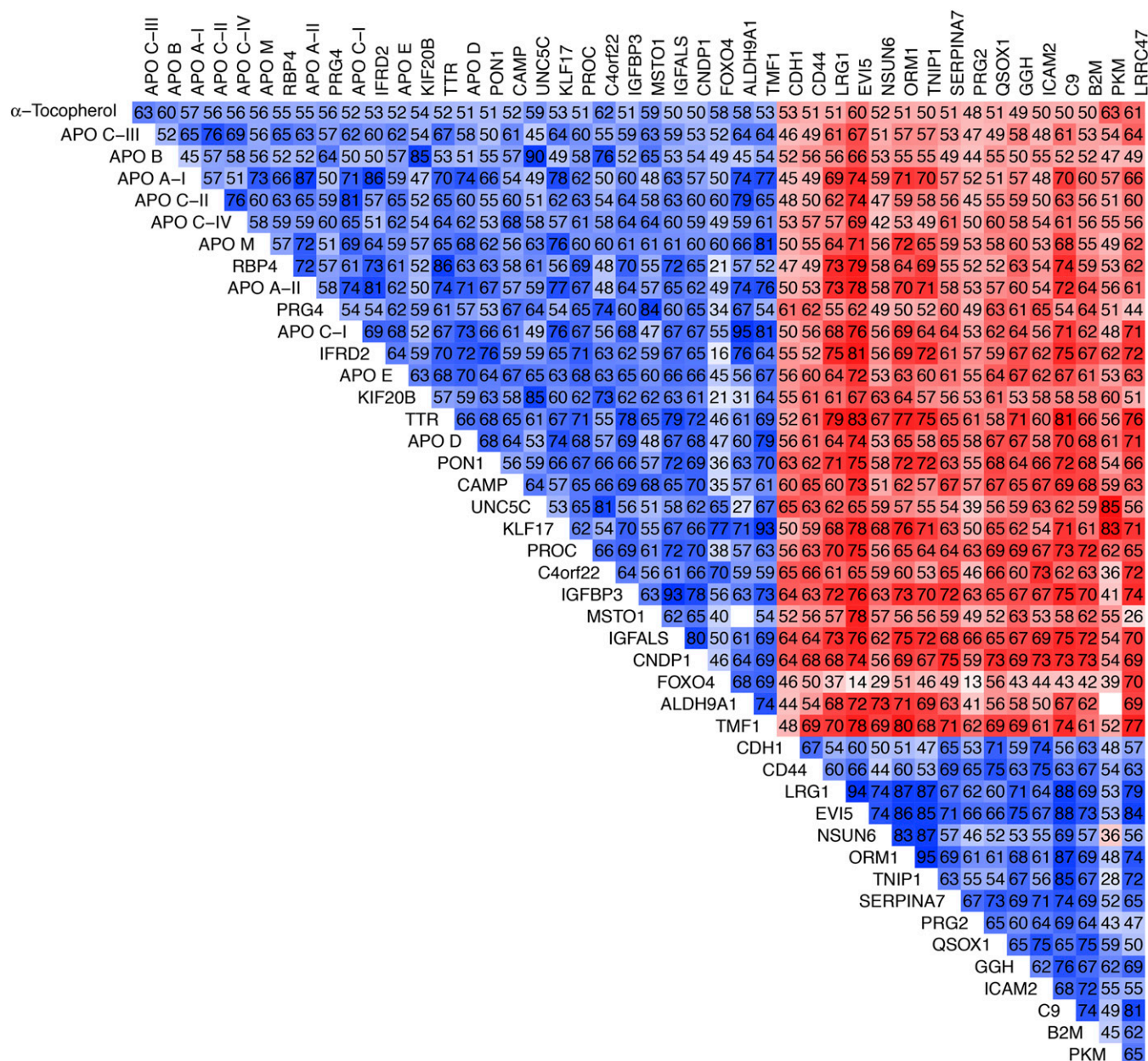


FIGURE 1 Matrix of correlation coefficients for pairs of LME-based estimates of relative abundance and plasma α -tocopherol concentration for proteins associated with α -tocopherol, restricted to associations with $q < 0.01$ ($n = 44$), in children of rural Nepal aged 6–8 y ($n = 500$). Blue depicts proteins that share a positive correlation, red shows a negative correlation, and darker colors represent a stronger association. All correlation coefficients (r) are presented as $r \times 10^2$ to improve visualization. Blank cells represent unobserved protein pairs in any of the same participants. ALDH9A1, aldehyde dehydrogenase 9A1; B2M, β -2-microglobulin; C4orf22, chromosome 4 open reading frame 22; C9, complement component 9; CD44, CD44 antigen isoform 4; CDH, cadherin 1, type 1; CNDP1, carnosine dipeptidase; EVI5, ecotropic viral integration site 5; FOXO4, forkhead box protein O4; GGH, γ -glutamyl hydrolase; ICAM2, intercellular adhesion molecule 2; IFRD2, interferon-related developmental regulator 2; IGFALS, insulin-like growth factor-binding protein, acid-labile subunit isoform 2; IGFBP3, insulin-like growth factor-binding protein 3 isoform b; KIF20B, kinesin-like protein KIF20B; KLF17, Kruppel-like factor 17; LME, linear mixed effects; LRG1, leucine-rich α -2-glycoprotein 1; LRRC47, leucine-rich repeat containing 47; MSTO1, Misato homolog 1; NSUN6, NOP2/Sun domain family, member 6; ORM1, orosomucoid 1; PKM, pyruvate kinase, muscle; PON1, paraoxonase 1; PRG2, proteoglycan 2; PRG4, proteoglycan 4 isoform D; PROC, protein C; QSOX1, quiescins Q6 sulfhydryl oxidase 1; RBP4, retinol-binding protein 4; SERPINA7, serpin peptidase inhibitor, clade A, member 7; TMF1, TATA element modulatory factor; TNIP1, TNFAIP-interacting protein 1; TTR, transthyretin; UNC5C, Unc5 homolog C.

Discussion

Vitamin E deficiency likely exists with health consequence (1–5) but remains latent and is thus largely ignored in most undernourished societies. Encouraged by an earlier finding of strong association between plasma α -tocopherol and apoC-III (7), this analysis sought to detect through quantitative proteomics a

cluster of biomarkers that could be modeled to predict α -tocopherol concentrations in a generally undernourished population. The public health utility of this discovery approach lies in its potential to guide the development of targeted, multi-protein quantification assays that may be able to simultaneously estimate the prevalence of multiple micronutrient deficiencies, including vitamin E, on a less costly, faster platform (e.g., using

TABLE 3 Stepwise LME model explaining variability in plasma α -tocopherol by candidate proteins in a plasma α -tocopherome children of rural Nepal aged 6–8 y ($n = 500$)¹

Protein name	HUGO gene symbol	Accession number ²	Model R^2	R^2 increment	Model AIC	AIC decrement ³
ApoC-III	<i>APOC3</i>	4557323	0.40	NA	2449	NA
ApoB	<i>APOB</i>	105990532	0.49	0.08	2388	–61
Pyruvate kinase, muscle	<i>PKM</i>	33286422	0.58	0.09	2306	–82
Forkhead box O4	<i>FOXO4</i>	103472003	0.64	0.06	2239	–67
Unc5 homolog (C. elegans)	<i>UNC5C</i>	16933525	0.67	0.03	2209	–30
Regulator of G-protein signaling 8	<i>RGS8</i>	156416024	0.71	0.04	2152	–56

¹ A multivariate model was chosen by generating candidate proteins based on a false discovery rate $<10\%$ ($q < 0.10$) and P value <0.0001 in their marginal association with plasma α -tocopherol. Candidate proteins had nonmissing values for all 500 samples that were derived from LME-adjusted iTRAQ mass spectrometry experiments or from multiple imputation modeling of missing values. The following 9 second-tier proteins (with corresponding HUGO gene symbols and GenInfo accession numbers listed in parentheses) may enhance the prediction of plasma α -tocopherol and merit future absolute quantification: alcohol dehydrogenase 9 family, member A1 (*ALDH9A1*, 115887104), apoM (*APOM*, gi22091452), cadherin 1, type 1 (*CDH1*, 4757960), CD44 antigen isoform 4 (*CD44*, 48255941), chromosome 4 open reading frame 22 (*C3orf22*, 2274509), kinesin-like protein KIF201B (*KIF20B*, 46049114), Misato 1 (*MSTO1*, 39780571), proteoglycan 4 isoform D (*PRG4*, 189181724), and quiescin Q6 sulfhydryl oxidase (*QSOX*, 13325075). AIC, Akaike information criterion; HUGO, Human Genome Organization; LME, linear mixed effects.

² GenInfo sequence number as assigned to all nucleotide and protein sequences by the National Center for Biotechnology Information at the National Library of Medicine, NIH (18).

³ Model building ceased on reaching an AIC decrement <30 .

antibody methods). To our knowledge, such a multinutrient proteomics system does not yet exist, but a first step toward achieving this potential is to discover, quantify, and evaluate protein candidates for such a system.

This study revealed a plasma α -tocopherome that consisted of 119 of 982 proteins in a population of Nepali children in whom vitamin E and other nutritional deficiencies, as well as inflammation, were common (4). Restricting admissible proteins to a false discovery rate $<10\%$ offered reasonable assurance against spurious associations of proteins with α -tocopherol, although 44 proteins also met a more stringent threshold of 1%. After imputing missing values for multivariable regression analysis and employing a stepwise method that limited the selection of proteins based on the strength of their contribution to predicting α -tocopherol, 6 proteins entered a model that explained 71% of the variation in plasma α -tocopherol and predicted an in-sample prevalence of vitamin E deficiency of 51%, which was similar to a prevalence of 54% based on α -tocopherol concentrations at a conventional cutoff of $<12 \mu\text{mol/L}$ (1, 26). Although promising, the unavailability of an independent population to retest the model merits caution in interpreting these results. Intriguingly, the 2 negative correlates in the model, PKM and RGS8, could be functional markers of depleted vitamin E nutriture. PKM, an intermediate of glycolysis, is known to be released from erythrocytes and other cells damaged by vitamin E deficiency (54), and RGS8, a cytosolic G-protein signaling regulator, concentrates in the Purkinje cells of the cerebellum (55), where neurological lesions of vitamin E deficiency seem to be most pronounced (56).

Although relative abundance estimation permits nutrient:protein pairs to be evaluated for direction, strength, and predictivity of association, absolute quantification of candidate proteins will be needed to test the ability of a protein-based model for predicting status and the prevalence of vitamin E deficiency. In addition, because the optimal model could vary across populations, including those populations that are better nourished, 9 additional proteins were identified that may be exchangeable or add power for predicting plasma α -tocopherol, thus increasing the number of candidate proteins to target for future absolute quantification.

Beyond prediction, a novel advantage of a plasma proteomics approach is the opportunity it affords for discovering plausible, functional suites of biomarkers associated with nutrient status. Criteria of plausibility of association include prior evidence of 1) direct nutrient:protein molecular interaction (e.g., in transport or biogenesis); 2) colocalization in which molecular linkages are likely, if not established [e.g., phospholipid-rich membranes for α -tocopherol (57)], or 3) covariation between the nutrient and metabolic systems in which associated proteins participate [e.g., immune (58), coagulative (59), or nervous (60–62) systems]. The first criterion is illustrated by α -tocopherol's lipid antioxidant (63, 64) and nonantioxidant roles in regulating gene expression, lipid metabolism (60–62), and membrane homeostasis and repair (64). Strong positive correlations of α -tocopherol with aposA (I, II), B, C (I–IV), E, and L likely reflect the vitamer's postabsorptive and hepatic release into circulation, where it admixes with virtually all lipoproteins (9, 10, 65). Positive correlation with some lipocalins (retinol-binding protein 4 and apos D and M) may similarly reflect the carriage of α -tocopherol with low-molecular-weight lipids transported by these proteins (27). However, correlations with lipid transporters may also represent comodulatory roles with α -tocopherol in cross-talking immune (66, 67), inflammatory (67–69), coagulative (70), and neurological (60, 61, 66) systems. In addition, the observed positive correlation between plasma α -tocopherol and the protein afamin, a multifunctional albumin-family glycoprotein, may reflect more remote interactions because although afamin transports α -tocopherol in extravascular fluids it does not do so in plasma (71).

In systematic terms, α -tocopherol attenuates inflammation by suppressing, for example, the expression of TNF- α , IL-1 β and -6, platelet aggregation, monocyte adhesion, and oxidative stress (58, 68, 72). These homeostatic influences may give rise to the vitamer's negative correlations with positive acute-phase reactants such as orosomucoid 1 and 2, ceruloplasmin (37), and lipocalin-2 (66), as well as effectors in complement activation (40), wound repair (39, 64), monocyte activation, and intercellular adhesion [cadherin 1, type 1 (44); intercellular and vascular cell-adhesion molecules (73); CD14 (42); desmoglein-2 (47); CD44 antigen isoform 4 (45); and vitamin D-binding

TABLE 4 Plasma proteins associated with plasma log₂ γ-tocopherol in children of rural Nepal aged 6–8 y (*n* = 500)¹

Protein name	HUGO gene				<i>P</i>	<i>q</i>	<i>b</i> ²	Accession number ³
	symbol	<i>n</i>	<i>r</i>	<i>R</i> ²				
ApoC-III ⁴	<i>APOC3</i>	500	0.32	0.10	2.56 × 10 ^{−6}	0.004	28.8	4557323
ApoA-IV	<i>APOA4</i>	500	0.31	0.10	1.11 × 10 ^{−5}	0.009	34.4	71773110
ApoC-IV	<i>APOC4</i>	500	0.31	0.10	1.80 × 10 ^{−5}	0.010	22.6	4502161
Serpin peptidase inhibitor, clade C (antithrombin), member 1	<i>SERPINC1</i>	500	−0.30	0.09	0.0002	0.067	−53.1	4502261
α-2-HS-glycoprotein	<i>AHSG</i>	500	−0.29	0.08	0.0003	0.067	−30.9	156523970
InaD-like (<i>Drosophila</i>)	<i>INADL</i>	271	−0.21	0.05	0.0003	0.067	−29.0	112382257
α-2-Macroglobulin	<i>A2M</i>	500	−0.29	0.09	0.0003	0.067	−44.3	66932947
Protein C (inactivator of coagulation factors Va and VIIIa)	<i>PROC</i>	500	0.29	0.08	0.0005	0.077	43.0	4506115
ApoB [including Ag(x) antigen]	<i>APOB</i>	500	0.29	0.08	0.0005	0.077	36.5	105990532
ApoA-I	<i>APOA1</i>	500	0.29	0.08	0.0008	0.093	39.5	4557321
Cathelicidin antimicrobial peptide	<i>CAMP</i>	417	0.31	0.10	0.0008	0.093	19.9	39753970
Misato homolog 1 ⁴	<i>MSTO1</i>	110	0.46	0.21	0.001	0.098	66.7	39780571

¹ Twelve proteins quantified by mass spectrometry and estimated by linear mixed-effects modeling in >10% of the samples (50 < *n* ≤ 500) that are correlated with plasma log₂ γ-tocopherol, subjected to a false discovery rate cutoff of 10% (*q* < 0.10), and listed in increasing order of *q* are defined as candidate protein biomarkers for a plasma γ-tocopherome.

² Percentage change in plasma γ-tocopherol (in μmol/L) per 100% increase in relative protein abundance.

³ GenInfo Identifier sequence number as assigned to all nucleotide and protein sequences by the National Center for Biotechnology Information at the National Library of Medicine, NIH (18).

⁴ Proteins included in a stepwise regression model that explained 20% of the variability in plasma γ-tocopherol concentration.

protein, which activates macrophages (38)]. Broad effects of α-tocopherol in the anticoagulant pathway may be expected to give rise to positive correlations with cytoprotective proteins C (31) and Z (32), which are thought to dampen coagulation cascades and prevent thrombosis.

Associations between α-tocopherol and some biomarkers of inflammation and coagulation may at first seem contradictory, such as a negative correlation with SERPINC1. This serine protease inhibitor exerts anti-inflammatory activity by inhibiting activation of the classic complement pathway and suppressing premature activation of downstream factors in the coagulation cascade (48). However, these actions require a rise in SERPINC1 abundance during the initial response to inflammation (48), potentially explaining the observed negative association with plasma α-tocopherol. Alternatively, positive correlations with enzymes that upregulate coagulation such as factors II (thrombin), VII, XI, XIII A1, and XIII B could reflect α-tocopherol's association with inactive zymogen precursors of these proteins that circulate in high abundance under noninflamed, homeostatic conditions. Associations of these types would be consistent with roles α-tocopherol may play in promoting readiness of the complement, coagulation and kinin-bradykinin systems to respond to challenges and, once activated, aiding to minimize tissue injury.

Many plasma α-tocopherome proteins localize to phospholipid-rich membranes of neural tissues, where α-tocopherol is abundant, neuroprotective, and maintains redox homeostasis (56, 60). Neural tissue is also where early lesions of vitamin E deficiency may occur (74), leading to the loss of neuromuscular function (60, 61). In a rare controlled therapeutic study, malnourished, vitamin E-deficient Indian children showed marked neurological improvement after 6 wk of vitamin E supplementation (75). In our study, plasma α-tocopherome biomarkers included proteins known to be involved in neuronal guidance [unc5 homolog C (34)]; neuromodulation [prostaglandin D2 synthase (76), apoA-1 (62), kininogen-1 (77), and lipocalin-2 (66)]; cilium and axonemal conformation, motility, attachment, and motor function [dynein, axonemal

assembly factor 1 (78), kinesin-like protein (33), Bardet-Biedl syndrome 7, and tubulin tyrosine ligase-like family, member 8 (78)]; cargo transfer, vesiculation, and cytosolic transport [clathrin (79), dynein (78), and kinesin isoforms (33)]; and redox homeostasis [peroxiredoxin-2 (52), thioredoxin (53), queiscin-sulfhydryl oxidase (51), paraoxonases (36), and selenoprotein P1 (29)], all functions required for neuromuscular health.

A far smaller, less significant, and nonpredictive plasma proteome was associated with plasma γ-tocopherol and comprised 12 proteins at a false discovery rate <10%, 8 of which also correlated with α-tocopherol. The striking differences between α- and γ-tocopheromes may reflect the extent to which the α-tocopherol transfer protein, synthesized in the liver and brain, actively facilitates the circulation of α-tocopherol to tissues to promote the functions ascribed to vitamin E (65).

In summary, an unbiased, quantitative proteomics approach identified 6 plasma proteins whose relative abundance explained sufficient variability in plasma α-tocopherol to predict with reasonable accuracy the in-sample prevalence of vitamin E deficiency. The study detected 119 protein correlates of vitamin E (a plasma α-tocopherome) of diverse function that can potentially serve as biomarkers of the physiological and disease processes associated with vitamin E deficiency. Next steps involve absolute quantification of targeted proteins, verification of their ability to predict vitamin E deficiency, migration of their measurement onto a simpler protein assay platform, and further testing in populations.

Acknowledgments

The Johns Hopkins nutripoteomics research team includes: Margia Arguello, Raghothama Chaerkady, Hongie Cui, Lauren R DeVine, Jaime Johnson, Robert O'Meally, Subarna K Khatri, Ashika Nanayakkara-Bind, Hee-Sool Rho, and Fredrick Van Dyke.

We thank Ingo Ruczinski for proteomics modeling and analytic guidance, C Conover Talbot Jr., for assistance with the Human Genome Organization gene annotation, and Cate Kiefe

for assistance with Figure 1. KPW, RNC, KJS, JDY, JDG, and PC designed the research; RNC, SS, and KJS performed the research; RNC, KJS, SEL, and JB contributed new reagents or analytic tools; JB, BASN, and LS-FW analyzed the data; KPW, LS-FW, and PC conducted the original field study; KPW, SS, KJS, and BASN wrote the manuscript; and KPW had primary responsibility for final content. All authors read and approved the final manuscript.

References

- Traber MG. Vitamin E inadequacy in humans: causes and consequences. *Adv Nutr* 2014;5:503–14.
- Dror DK, Allen LH. Vitamin E deficiency in developing countries. *Food Nutr Bull* 2011;32:124–43.
- Jiang T, Christian P, Khatry SK, Wu L, West KP, Jr. Micronutrient deficiencies in early pregnancy are common, concurrent, and vary by season among rural Nepali pregnant women. *J Nutr* 2005;135:1106–12.
- Schulze KJ, Christian P, Wu LS-F, Arguello M, Cui H, Nanayakkara-Bind A, Stewart C, Khatry SK, LeClerq S, West KP, Jr. Micronutrient deficiencies are common in 6- to 8-year-old children of rural Nepal, with prevalence estimates modestly affected by inflammation. *J Nutr* 2014;144:979–87.
- Shamim AA, Schulze KJ, Merrill RD, Kabir A, Christian P, Shaikh S, Wu L, Ali H, Labrique AB, Mehra S, et al. First trimester plasma tocopherols are associated with risk of miscarriage in rural Bangladesh. *Am J Clin Nutr* 2015;101:294–301.
- Raiten DJ, Ashour FA, Ross AC, Meydani SN, Dawson HD, Stephens CB, Brabin BJ, Suchdev PS, van Ommen B. Inflammation and nutritional science for programs/policies and interpretation of research evidence (INSPIRE). *J Nutr* 2015;145:1039S–108S.
- Cole RN, Ruczinski I, Schulze K, Christian P, Herbrich S, Wu L, DeVine LR, O'Meally RN, Shrestha S, Boronina TN, et al. The plasma proteome identifies expected and novel proteins correlated with micronutrient status in undernourished Nepalese children. *J Nutr* 2013;143:1540–8.
- Herbrich SM, Cole RN, West KP, Jr., Schulze K, Yager JD, Groopman JD, Christian P, Wu L, O'Meally RN, May DH, et al. Statistical inference from multiple iTRAQ experiments without using common reference standards. *J Proteome Res* 2013;12:594–604.
- Mendivil CO, Zheng C, Furtado J, Lel J, Sacks FM. Metabolism of very-low-density lipoprotein and low-density lipoprotein containing apolipoprotein C-III and not other small apolipoproteins. *Arterioscler Thromb Vasc Biol* 2010;30:239–45.
- Kayden HJ, Traber MG. Absorption, lipoprotein transport, and regulation of plasma concentrations of vitamin E in humans. *J Lipid Res* 1993;34:343–58.
- Da Costa LA, Garcia-Bailo B, Borchers CH, Badawi A, El-Sohehy A. Association between the plasma proteome and plasma α -tocopherol concentrations in humans. *J Nutr Biochem* 2013;24:396–400.
- Christian P, Khatry SK, Katz J, Pradhan EK, LeClerq SC, Shrestha SR, Adhikari RK, Sommer A, West KP, Jr. Effects of alternative maternal micronutrient supplements on low birth weight in rural Nepal: double blind randomized community trial. *BMJ* 2003;326:571–7.
- Stewart CP, Christian P, Schulze KJ, LeClerq SC, West KP, Jr., Khatry SK. Antenatal micronutrient supplementation reduces metabolic syndrome in 6- to 8-year-old children in rural Nepal. *J Nutr* 2009;139:1575–81.
- Stewart CP, Christian P, LeClerq SC, West KP, Jr., Khatry SK. Antenatal supplementation with folic acid + iron + zinc improves linear growth and reduces peripheral adiposity in school-age children in rural Nepal. *Am J Clin Nutr* 2009;90:132–40.
- Christian P, Murray-Kolb L, Khatry SK, Katz J, Schaefer BA, Cole PM, LeClerq SC, Tielsch M. Prenatal micronutrient supplementation and intellectual and motor function in early school-aged children in Nepal. *JAMA* 2010;304:2716–23.
- Yamini S, West KP, Jr., Wu L, Dreyfuss ML, Yang DX, Khatry SK. Circulating levels of retinol, tocopherol and carotenoid in Nepali pregnant and postpartum women following long-term beta-carotene and vitamin A supplementation. *Eur J Clin Nutr* 2001;55:252–9.
- Storey JD. A direct approach to false discovery rates. *J R Stat Soc B* 2002;64:479–98.
- National Center for Biotechnology Information. Genetic sequence data bank [Internet]. Bethesda (MD): National Library of Medicine (US). c2015 [cited 2015 Apr 15]. Available from: <ftp://ftp.ncbi.nih.gov/genbank/gbrel.txt>.
- National Center for Biotechnology Information. Sequence identifiers: an historical note [Internet]. Bethesda (MD): National Library of Medicine (US). c2004 [cited 2015 May 26]. Available from: <http://www.ncbi.nlm.nih.gov/Sitemap/sequenceIDs.html>.
- Little RJA, Rubin DB. Statistical analysis with missing data. 2nd ed. New York: John Wiley; 2002.
- Stone M. An asymptotic equivalence of choice of model by cross-validation and Akaike's criterion. *J R Stat Soc B* 1977;39:44–7.
- Kuhn M, Johnson K. Applied predictive modelling. New York: Springer; 2013.
- The Comprehensive R Archive Network [Internet]. Vienna (Austria): Institute for Statistics and Mathematics, Vienna University of Economics and Business. c2004 [cited 2015 May 27]. Available from: <http://cran.r-project.org>.
- WHO. Growth reference data for 5–19 years [Internet]. Geneva (Switzerland): WHO. c2007 [cited 2015 Jan 3]. Available from: <http://www.who.int/growthref/en>.
- Campbell RK, Talegawkar SA, Christian P, LeClerq SC, Khatry SK, Wu LS-F, West KP, Jr. Seasonal dietary intakes and socioeconomic status among women in the Terai of Nepal. *J Health Pop Nutr* 2014;32:198–216.
- Institute of Medicine. Vitamin E. In: Dietary reference intakes for vitamin A, vitamin E, selenium, and carotenoids. Washington (DC): National Academy Press; 2000. p. 186–283.
- Perdomo G, Kim DH, Zhang T, Qu S, Thomas EA, Toledo FGS, Slusher S, Fan Y, Kelley DE, Dong HH. A role of apolipoprotein D in triglyceride metabolism. *J Lipid Res* 2010;51:1298–311.
- Liz MA, Faro CF, Saraiva MJ, Sousa MM. Transthyretin, a new cryptic protease. *J Biol Chem* 2004;279:21431–8.
- Burk RF, Hill KE. Selenoprotein P-expression, functions, and roles in mammals. *Biochim Biophys Acta* 2009;1790:1441–7.
- Bucki R, Leszczynska K, Namiot A, Sokołowski W. Cathelicidin LL-37: a multitask antimicrobial peptide. *Arch Immunol Ther Exp (Warsz)* 2010;58:15–25.
- Bouwens EAM, Stavenhagen F, Mosnier LO. Mechanisms of anticoagulant and cytoprotective actions of the protein C pathway. *J Thromb Haemost* 2013;11:242–53.
- Almawi WY, Al-Shaikh FS, Melemedjian OK, Almawi AW. Protein Z, an anticoagulant protein with expanding role in reproductive biology. *Reproduction* 2013;146:R73–80.
- Janisch KM, Vock VM, Fleming MS, Shrestha A, Grimsley-Myers CM, Rasoul BA, Neale SA, Cupp TD, Kinchen JM, Liem KF, Jr., et al. The vertebrate-specific Kinesin-6, Kif20b, is required for normal cytokinesis of polarized cortical stem cells and cerebral cortex size. *Development* 2013;140:4672–82.
- Kim D, Ackerman SL. The UNC5C netrin receptor regulates dorsal guidance of mouse hindbrain axons. *J Neurosci* 2011;31:2167–79.
- Fleming CE, Mar FM, Franquinhof F, Sousa MM. Transthyretin: an enhancer of nerve generation. *Int Rev Neurobiol* 2009;87:337–46.
- Camps J, Garcia-Heredia A, Rull A, Alonso-Villaverde C, Aragones G, Beltran-Debon R, Rodriguez-Gallego E, Joven J. PPARs in regulation of paraoxonases: control of oxidative stress and inflammation pathways. *PPAR Research* [Internet] 2012. Available from: <http://www.hindawi.com/journals/ppar/2012/616371>.
- Hellman NE, Gitlin JD. Ceruloplasmin metabolism and function. *Annu Rev Nutr* 2002;22:439–58.
- Speeckaert M, Huang G, Delanghe JR, Taes YEC. Biological and clinical aspects of the vitamin D binding protein (Gc-globulin) and its polymorphism. *Clin Chim Acta* 2006;372:33–42.
- Bryckaert M, Rosa J-P, Denis CV, Lenting PJ. Of von Willebrand factor and platelets. *Cell Mol Life Sci* 2015;72:307–26.
- Mayilyan KR. Complement genetics, deficiencies, and disease associations. *Protein Cell* 2012;3:487–96.
- Hochepied T, Berger FG, Baumann H, Libert C. α 1-Acid glycoprotein: an acute phase protein with inflammatory and immunomodulating properties. *Cytokine Growth Factor Rev* 2003;14:25–34.

42. Plóciennikowska A, Hromada-Judycka A, Borzecka K, Kwiatowska K. Cooperation of TLR4 and raft proteins in LPS-induced inflammatory signaling. *Cell Mol Life Sci* 2015;72:557–81.
43. Li MO, Wan YY, Sanjabi S, Robertson A-KL, Flavell RA. Transforming growth factor- β regulation of immune responses. *Annu Rev Immunol* 2006;24:99–146.
44. Schneider MR, Kolligs FT. E-cadherin's role in development, tissue homeostasis and disease: Insights from mouse models: Tissue-specific inactivation of the adhesion protein E-cadherin in mice reveals its functions in health and disease. *BioEssays* 2015;37:294–304.
45. Bajorath J. Molecular organization, structural features, and ligand binding characteristics of CD44, a highly variable cell surface glycoprotein with multiple functions. *Proteins* 2000;39:103–11.
46. Halai K, Whiteford J, Ma B, Nourshargh S, Woodfin A. ICAM-2 facilitates luminal interactions between neutrophils and endothelial cells in vivo. *J Cell Sci* 2014;127:620–9.
47. Nekrasova OE, Amargo EV, Smith WO, Chen J, Kreitzer GE, Green KJ. Desmosomal cadherins utilize distinct kinesins for assembly into desmosomes. *J Cell Biol* 2011;195:1185–203.
48. Bossi F, Peerschke EI, Ghebrehiwet B, Tedesco F. Cross-talk between the complement and the kinin system in vascular permeability. *Immunol Lett* 2011;140:7–13.
49. Kalsheker NA. a,-antichymotrypsin. *Int J Biochem Cell Biol* 1996;28:961–4.
50. Nielsen MJ, Moller HJ, Moestrup SK. Hemoglobin and heme scavenger receptors. *Antioxid Redox Signal* 2010;12:261–73.
51. Kodali VK, Thorpe C. Oxidative protein folding and the quiescin-sulfhydryl oxidase family of flavoproteins. *Antioxid Redox Signal* 2010;13:1217–30.
52. Low FM, Hampton MB, Winterbourn CC. Peroxiredoxin 2 and peroxide metabolism in the erythrocyte. *Antioxid Redox Signal* 2008;10:1621–30.
53. Nordberg J, Arner ES. Reactive oxygen species, antioxidants, and the mammalian thioredoxin system. *Free Radic Biol Med* 2001;31:1287–312.
54. Barella L, Muller PY, Schlachter M, Hunziker W, Stocklin E, Spitzer V, Meier N, de Pascual-Teresa S, Minihane AM, Rimbach G. Identification of hepatic molecular mechanisms of action of alpha-tocopherol using global gene expression profile analysis in rats. *Biochim Biophys Acta* 2004;1689:66–74.
55. Itoh M, Odagiri M, Abe H, Saitoh O. RGS8 protein is distributed in dendrites and cell body of cerebellar Purkinje cell. *Biochem Biophys Res Commun* 2001;287:223–8.
56. Ulatowski L, Parker R, Warriar G, Sultana R, Butterfield DA, Manor D. Vitamin E is essential for Purkinje neuron integrity. *Neuroscience* 2014;260:120–9.
57. Marquardt D, Williams JA, Kucerka N, Atkinson J, Wassall SR, Katsaras J, Harroun TA. Tocopherol activity correlates with its location in a membrane: a new perspective on the antioxidant vitamin E. *J Am Chem Soc* 2013;135:7523–33.
58. Reiter E, Jiang Q, Christen S. Anti-inflammatory properties of α - and γ -tocopherol. *Mol Aspects Med* 2007;28:668–91.
59. de Maat S, de Groot PG, Maas C. Contact system activation on endothelial cells. *Semin Thromb Hemost* 2014;40:887–94.
60. Gohil K, Vasu VT, Cross CE. Dietary α -tocopherol and neuromuscular health: search for optimal dose and molecular mechanisms continues. *Mol Nutr Food Res* 2010;54:693–709.
61. Ulatowski L, Manor D. Vitamin E trafficking in neurologic health and disease. *Annu Rev Nutr* 2013;33:87–103.
62. Meyers L, Groover C, Douglas J, Lee S, Brand D, Levin MC, Gardner LA. A role for apolipoprotein A-1 in the pathogenesis of multiple sclerosis. *J Neuroimmunol* 2014;277:176–85.
63. Traber MG, Stevens JF. Vitamins C and E: beneficial effects from a mechanistic perspective. *Free Radic Biol Med* 2011;51:1000–13.
64. Howard AC, McNeil AK, McNeil PL. Promotion of plasma membrane repair by vitamin E. *Nature Comm* 2011;2:597.
65. Traber MG. Vitamin E regulatory mechanisms. *Annu Rev Nutr* 2007;27:347–62.
66. Jha MK, Lee S, Park DH, Kook H, Park K, Lee I, Suk K. Diverse functional roles of lipocalin-2 in the central nervous system. *Neurosci Biobehav Rev* 2015;49:135–56.
67. Singh U, Devaraj S, Jialal I. Vitamin E, oxidative stress and inflammation. *Annu Rev Nutr* 2005;25:151–74.
68. Glauert HP. Vitamin E and NF- κ B activation: a review. *Vitam Horm* 2007;76:135–53.
69. Huang Z-G, Liang C, Han S-F, Wu Z-G. Vitamin E ameliorates ox-LDL-induced foam cells formation through modulating the activities of oxidative stress-induced NF- κ B pathway. *Mol Cell Biochem* 2012;363:11–9.
70. Ricciarelli R, Zingg JM, Azzi A. Vitamin E: protective role of a Janus molecule. *FASEB J* 2001;15:2314–25.
71. Jerkovic L, Voegelé AF, Chwatal S, Kronenberg F, Radcliffe CM, Wormald MR, Lobentanz EM, Ezech B, Eller P, Dejori N, et al. Afamin is a novel human vitamin E-binding glycoprotein characterization and in vitro expression. *J Proteome Res* 2005;4:889–99.
72. Freedman JE, Keaney JF. Vitamin E inhibition of platelet aggregation is independent of antioxidant activity. *J Nutr* 2001;131:374S–7S.
73. Desideri G, Marinucci C, Tomassoni G, Masci PG, Sanatucci A, Ferri C. Vitamin E supplementation reduces plasma vascular cell adhesion molecule-1 and von Willebrand Factor levels and increases nitric oxide concentrations in hypercholesterolemic patients. *J Clin Endocrinol Metab* 2002;87:2940–5.
74. Fukui K, Masuda A, Hosono A, Suwabe R, Yamashita K, Shinkai T, Urano S. Changes in microtubule-related proteins and autophagy in long-term vitamin E-deficient mice. *Free Radic Res* 2014;48:649–58.
75. Kalra V, Grover JK, Ahuja GK, Rath S, Gulani S, Kalra N. Vitamin E administration and reversal of neurological deficits in protein-energy malnutrition. *J Trop Pediatr* 2001;47:39–45.
76. Liu H, Li W, Rose ME, Pascoe JL, Miller TM, Ahmada M, Poloyac SM, Hickey WR, Graham SH. Prostaglandin D2 toxicity in primary neurons is mediated through its bioactive cyclopentenone metabolites. *Neurotoxicology* 2013;39:35–44.
77. Guevara-Lora I. Kinin-mediated inflammation in neurodegenerative disorders. *Neurochem Int* 2012;61:72–8.
78. Panayotis N, Karpova A, Kreutz MR, Fainzilber M. Macromolecular transport in synapse to nucleus communication. *Trends Neurosci* 2015;38:108–16.
79. Traub LM. Common principles in clathrin-mediated sorting at the Golgi and the plasma membrane. *Biochim Biophys Acta* 2005;1744:415–37.